

## An adaptive loop gain selection for CLEAN deconvolution algorithm

Li Zhang<sup>1</sup>, Long Xu<sup>2</sup>, Ming Zhang<sup>3,4</sup> and Zhong-Zu Wu<sup>5</sup>

<sup>1</sup> College of Big Data and Information Engineering, Guizhou University, Guiyang 550025, China;  
[lizhang.science@gmail.com](mailto:lizhang.science@gmail.com)

<sup>2</sup> Key Laboratory of Solar Activity, National Astronomical Observatories, Chinese Academy of Sciences, Beijing 100101, China

<sup>3</sup> Xinjiang Astronomical Observatory, Chinese Academy of Sciences, Urumqi 830011, China

<sup>4</sup> Key Laboratory of Radio Astronomy, Chinese Academy of Sciences, Urumqi 830011, China

<sup>5</sup> College of Physics, Guizhou University, Guiyang 550025, China

Received 2018 July 29; accepted 2018 November 31

**Abstract** Radio interferometry significantly improves the resolution of observed images, and the final result also relies heavily on data recovery. The Cotton-Schwab CLEAN (CS-Clean) deconvolution approach is a widely used reconstruction algorithm in the field of radio synthesis imaging. However, parameter tuning for this algorithm has always been a difficult task. Here, its performance is improved by considering some internal characteristics of the data. From a mathematical point of view, a peak signal-to-noise-based (PSNR-based) method was introduced to optimize the step length of the steepest descent method in the recovery process. We also found that the loop gain curve in the new algorithm is a good indicator of parameter tuning. Tests show that the new algorithm can effectively solve the problem of oscillation for a large fixed loop gain and provides a more robust recovery.

**Key words:** methods: data analysis — techniques: image processing — techniques: interferometric

### 1 INTRODUCTION

Radio interferometry enables high-resolution observations by combining multiple telescopes at different locations to achieve sampling in the spatial frequency domain, e.g. at VLA<sup>1</sup> and ALMA<sup>2</sup>. However, radio interferometry cannot satisfy the Nyquist sampling theorem in the spatial frequency domain in most cases, which is equivalent to introducing a blur kernel into the spatial domain. In the field of radio astronomy, a blur kernel and a blur image are often referred to as a dirty beam (or point spread function, PSF) and dirty image, respectively (Thompson et al. 2017). The effect of a dirty beam needs to be removed from the dirty image to obtain the latent true image.

CLEAN deconvolution is widely employed in the processing of radio interferometric data and it has become the standard implementation in almost all radio interferometric data processing softwares. Many CLEAN deconvolution

algorithms have been proposed to solve problems such as the approximation of scale information: scale-less CLEAN algorithms (Högbom 1974; Clark 1980; Schwab & Cotton 1983), multi-scale CLEAN algorithms (Cornwell 2008; Rau & Cornwell 2011) and adaptive-scale CLEAN algorithms (Bhatnagar & Cornwell 2004; Zhang et al. 2016a,b). However, loop gain in the Cotton-Schwab Clean (CS-Clean) algorithm always uses a fixed empirical value during a deconvolution. If the loop gain is not within the range of empirical values, then deconvolution may be very slow, or oscillating or non-convergent (Thompson et al. 2017). If the loop gain is too small, the deconvolution process becomes slow and can also cause arithmetic errors due to repeated subtractions (Steer et al. 1984). If the loop gain is too large, then deconvolution will oscillate or diverge. Another problem is that a more suitable loop gain in the CS-Clean algorithm is found through several experiments and there is no accurate ‘indicator’ to guide the selection of loop gain in the different deconvolution methods. In this article, a new algorithm (which we call Robust CLEAN)

---

<sup>1</sup> <http://www.vla.nrao.edu/>

<sup>2</sup> <http://www.almaobservatory.org/>

is proposed to solve these two problems to achieve a more robust recovery.

## 2 CLEAN ALGORITHM

Radio interferometric data (spatial coherence function or visibility function)  $\mathbf{V}^{\text{true}}$  are measured in the spatial frequency domain. By the van Cittert-Zernike theorem (Thompson et al. 2017), the relation between the visibility function  $\mathbf{V}^{\text{true}}$  and latent true spatial distribution (image)  $\mathbf{I}^{\text{true}}$  is as follows

$$\mathbf{V}^{\text{true}}(u, v) = \int \int_{-\infty}^{+\infty} \mathbf{I}^{\text{true}}(l, m) e^{2\pi i(ul+vm)} dl dm, \quad (1)$$

where  $(u, v)$  and  $(l, m)$  are the coordinates of spatial frequency domain and spatial domain respectively. This is a complete sampling of the spatial frequency domain. However, in real measurements, the sampling is incomplete and noisy,

$$\mathbf{I}^{\text{dirty}} = \mathbf{F}(\mathbf{S}(\mathbf{V}^{\text{true}} + \mathbf{n}_f)), \quad (2)$$

where  $\mathbf{I}^{\text{dirty}}$  is the dirty image which is the Fourier transform of the measured visibility data,  $\mathbf{F}$  is the Fourier transform operator,  $\mathbf{S}$  is the sampling pattern and  $\mathbf{n}_f$  represents total noise and error such as from the receiver system. By the convolution theorem, the dirty image  $\mathbf{I}^{\text{dirty}}$  is a convolution of the dirty beam  $\mathbf{B}$  with the latent true distribution and noise

$$\mathbf{I}^{\text{dirty}} = \mathbf{B} * \mathbf{I}^{\text{model}} + \mathbf{B} * \mathbf{n}, \quad (3)$$

where  $\mathbf{I}^{\text{model}}$  is the model image, the symbol  $*$  denotes the convolution operator and  $\mathbf{n}$  is spatial noise.

In the CLEAN deconvolution framework, the latent true distribution is represented as

$$\mathbf{I}^{\text{true}} = \mathbf{I}^{\text{model}} + \epsilon = \sum_{k=0}^N \mathbf{I}_k^{\text{comp}}(\mathbf{p}_k) + \epsilon, \quad (4)$$

where  $\mathbf{I}_k^{\text{comp}}(\mathbf{p}_k)$  is a model component,  $N$  is the number of model components,  $\mathbf{p}_k$  are some parameters of model components, and  $\epsilon$  is the difference between the model image  $\mathbf{I}^{\text{model}}$  and the latent true distribution  $\mathbf{I}^{\text{true}}$ . Some commonly used models are a set of delta functions or Gaussian functions. A set of delta functions is used as a model in the CS-Clean algorithm, and the corresponding model and parameters are

$$\mathbf{I}_k^{\text{comp}} = a_k \delta(x - x_k), \quad (5)$$

where  $a_k$  and  $\delta(x - x_k)$  are the amplitude of the model component and the delta function at the position  $x_k$ , respectively. So, the amplitude  $a_k$  is the only parameter that can be adjusted by users in a delta function model.

In the spatial domain, CS-Clean deconvolution is equivalent to minimizing  $\chi^2$  to find the optimal solution

$$\chi^2 = \left\| \mathbf{I}^{\text{dirty}} - \mathbf{B} * \sum_k \mathbf{I}_k^{\text{comp}} \right\|_2^2, \quad (6)$$

where  $\|\cdot\|_2$  is the  $l_2$  norm. The  $\chi^2$  gradient is computed to find the updated direction in the steepest descent method

$$\begin{aligned} \frac{\partial \chi^2}{\partial \mathbf{p}_k} &= -2 \frac{\partial}{\partial \mathbf{p}_k} (\mathbf{I}^{\text{dirty}} - \mathbf{B} * \sum_k \mathbf{I}_k^{\text{comp}}) \\ &= -2 \frac{\partial}{\partial \mathbf{p}_k} (\mathbf{I}_k^{\text{residual}}), \end{aligned} \quad (7)$$

$$\begin{aligned} \frac{\partial \chi^2}{\partial a_k} &= -2 \frac{\partial \chi^2}{\partial a_k} = -2 \frac{\partial}{\partial a_k} (\mathbf{I}_k^{\text{residual}}) \\ &= -2 \mathbf{B} * [\mathbf{I}^{\text{residual}}]_k, \end{aligned} \quad (8)$$

where

$$[\mathbf{I}^r]_k = \max \left| \mathbf{I}^{\text{dirty}} - \mathbf{B} * \sum_k \mathbf{I}_k^{\text{comp}} \right|. \quad (9)$$

Here  $k$  is the ordinal of a component,  $|\cdot|$  is an absolute value operator and  $[\mathbf{I}^{\text{residual}}]_k$  is the peak value of the residual image  $\mathbf{I}_k^{\text{residual}}$ . We know from Equation (8) that the residual image offers the updated direction in the search space. The deconvolution algorithm finds the peak in the residual image, which is equivalent to getting the updated direction along the axis with the largest derivative.

The model is updated by

$$\mathbf{I}_{k+1}^{\text{model}} = \mathbf{I}_k^{\text{model}} + g a_k^{\text{ap}} \delta(x - x_k), \quad (10)$$

where  $\mathbf{I}_k^{\text{model}}$  is the model image composed of  $k$  components,  $0 < g < 1$ ,  $a_k^{\text{ap}}$  is the peak value of the current residual image and  $a_k = g a_k^{\text{ap}}$ . So, the loop gain  $g$  becomes the only adjustable parameter. At present, the value of  $g$  is empirical and generally recommended from 0.01 to 0.25 (Thompson et al. 2017). As mentioned above, some problems may occur when the loop gain is not appropriate. These problems can be solved effectively by more accurately estimating model components.

## 3 THE NEW ALGORITHM

An improper loop gain actually causes inappropriate model components to be subtracted. A method based on the PNSRs of residual images is introduced to solve this problem. The dirty image and residual images of intermediate steps actually contain two parts: the ‘signal’ term

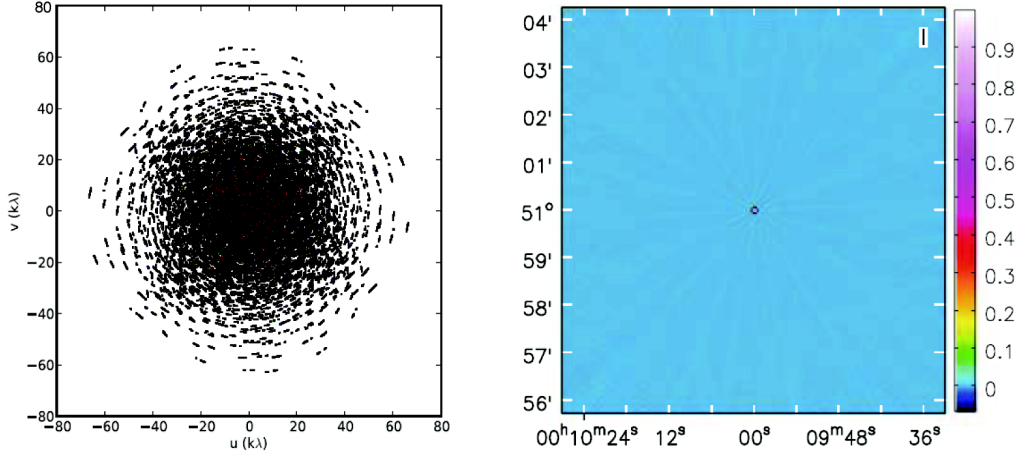


**Fig. 1** Left:  $uv$  coverage, right: Robustly-weighted PSF has a range of  $-0.068$  to  $1.0$  that is shown by logarithmic scaling (CASA scaling power cycles =  $-1.6$ ).

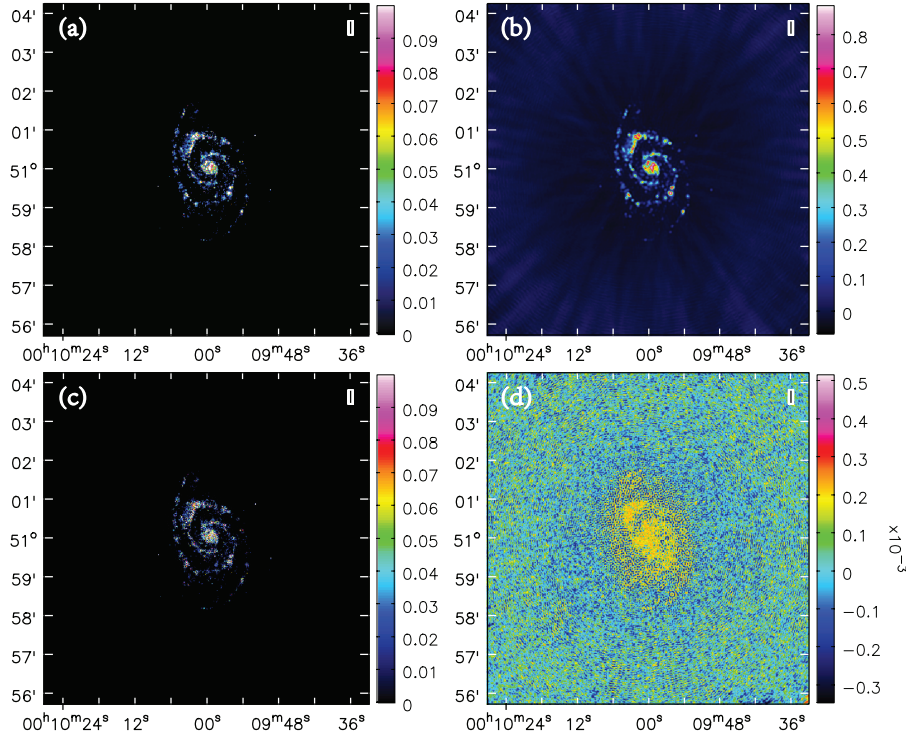


**Fig. 2** Deconvolution results from a radio image of M51: (a) the true image, (b) the dirty image, (c) the restored image from the new algorithm with  $g = 0.6$ , (d) the corresponding residual image.

$(\mathbf{B} * \mathbf{I}^{\text{model}})$  and the ‘noise’ term  $(\mathbf{B} * \mathbf{n})$ . The peak signal to noise ratio (PSNR) of a residual image (or a dirty image) is defined as follows

$$\text{PSNR} = 10 \lg \left( \frac{|m_n|}{\sigma} \right), \quad (11)$$

where  $\lg$  is the base 10 logarithmic function,  $m_n$  is the absolute maximum value of the residual image (or dirty image) and  $\sigma$  is the noise mean squared error from the noise

term of the dirty image. In the new algorithm, the loop gain  $g$  is adaptive with the change of PSNR from the current residual image. It is proportional to the ratio of the PSNR in the current residual image ( $\text{PSNR}_n$ ) to the PSNR of the dirty image ( $\text{PSNR}_0$ )

$$g = \begin{cases} k \frac{\text{PSNR}_n}{\text{PSNR}_0}, & k \frac{\text{PSNR}_n}{\text{PSNR}_0} \geq a \\ a, & k \frac{\text{PSNR}_n}{\text{PSNR}_0} < a \end{cases}, \quad (12)$$

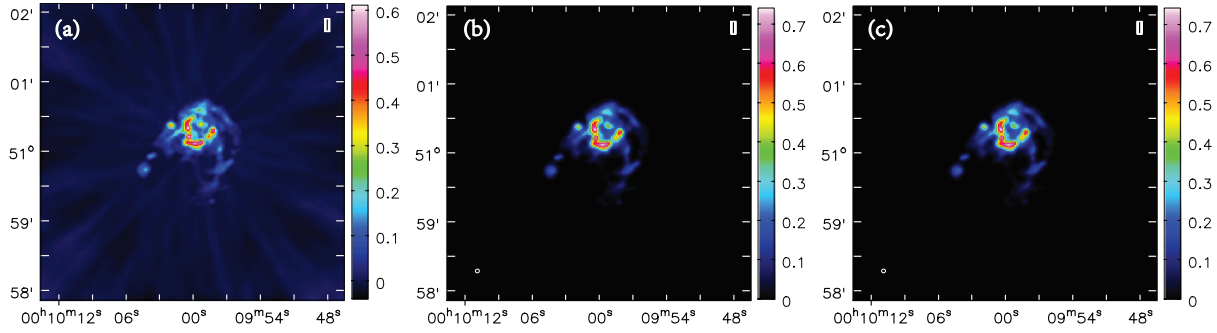


**Fig. 3** Deconvolution results from a radio image of M31: (a) the dirty image, (b) the restored image from the CS-Clean algorithm, (c) the restored image from the new algorithm with  $k = 0.6$ .

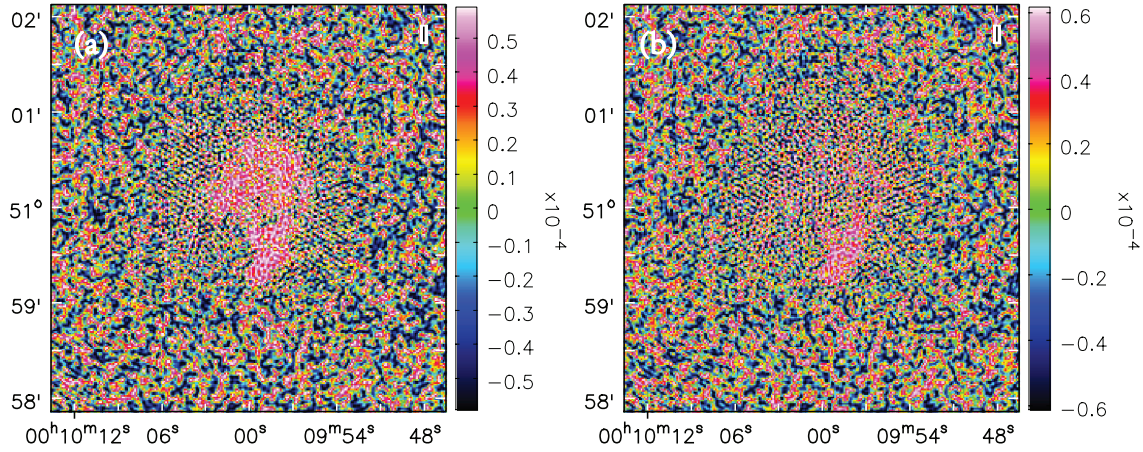


**Fig. 4** Deconvolution results from a radio image of M31: (a) the residual image from the CS-Clean algorithm, (b) the residual image from the new algorithm with  $k = 0.6$ .

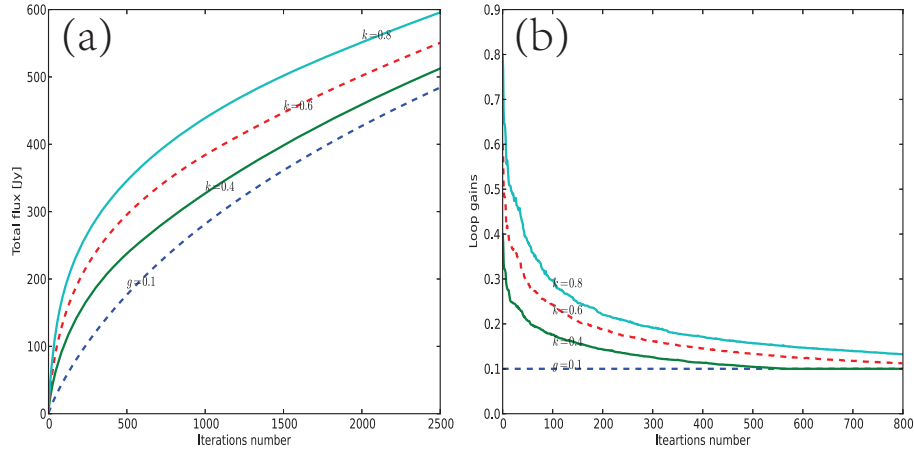


**Fig. 5** This figure shows some results from a radio image of M31. (a) The reconstruction speed of model flux is displayed with iteration number and different  $k$  values 0.4, 0.6 and 0.8, and is compared with fixed loop gain  $g = 0.1$ ; (b) the change of loop gain with iteration number and different  $k$  values 0.4, 0.6 and 0.8, and compares with fixed loop gain  $g = 0.1$ .

where  $0 < k \leq 1.0$ ; obviously  $0 < g \leq 1.0$  and  $a$  is a threshold.  $g = 1.0$  at the first iteration only when  $k = 1.0$ ; and  $k$  is used to estimate other factors such as extended features. If  $k \frac{\text{PSNR}_n}{\text{PSNR}_0}$  is less than a certain threshold, then this threshold will be used as the loop gain in subsequent

iterations. This strategy can avoid a time-consuming deconvolution caused by too small loop gains. To optimize this reconstruction problem, other factors such as the degree of extension of a radio source need to be considered. Here, these factors are included into this parameter  $k$ . In

other words,  $k$  is an overall representation of these factors (or these priors). We have found that this algorithm works well when  $0.1 \leq k \leq 0.6$  and  $a \leq 0.1$ .

The motivation for this method is as follows: the measured data always contain noise due to factors such as the receiving system. A dirty image is a combination of signal and noise. For the given measured data, the noise is fixed. Therefore, at the beginning of the deconvolution, signal is strong and the PSNR is large. At this point, the loop gain should be a large value. As the number of deconvolution iterations increases, some signals are removed and the PSNR of the current residual image becomes smaller. Then, a small loop gain is advisable.

Combining Equations (11) and (12),  $g$  can be simplified as follows

$$g = \begin{cases} k \frac{\lg |m_n| - \lg \sigma}{\lg |m_0| - \lg \sigma} & k \frac{\lg |m_n| - \lg \sigma}{\lg |m_0| - \lg \sigma} \geq a \\ a & k \frac{\lg |m_n| - \lg \sigma}{\lg |m_0| - \lg \sigma} < a \end{cases}, \quad (13)$$

where  $m_n$  and  $m_0$  are the peak values of the current residual image and the dirty image, respectively.  $\lg \sigma$  is fixed for a given image, so Equation (13) indicates that when  $k \frac{\lg |m_n| - \lg \sigma}{\lg |m_0| - \lg \sigma} \geq a$ , loop gains are proportional to the absolute maximum value of the current residual image. Therefore, a loop gain curve, which is a function of loop gains and the number of iterations, not only shows that loop gains change with the number of iterations, but also reveals the change of signal amplitude in a deconvolution process. Obviously, a loop gain curve that corresponds to a good reconstruction should be a monotonically non-increasing function. If the loop gain curve oscillates, it indicates that some of the model components are overestimated and a smaller  $k$  should be used. With the help of a loop gain curve, the parameter adjustment becomes easier. If the loop gain curve is strongly associated with the model image and residual image, then a parameter adjustment may be a better option. A loop gain curve can guide users to make more accurate adjustments to parameters.

#### 4 NUMERICAL EXPERIMENT

To illustrate the performance of the new algorithm, CASA software<sup>3</sup> was used to simulate the Expanded VLA (EVLA) in B configuration to observe two radio images (M51 and M31) for 6 hours in the L-band at 1 GHz and 32 channels. The corresponding  $uv$  coverage is shown in the left part of Figure 1. The measured visibilities contain Gaussian noise, which makes the dirty image have a noise level of root mean square (RMS)  $5.0 \times 10^{-5}$  Jy. The

main lobe width of the dirty beam is about 2 arcsec and the image resolution is 1 arcsec. Robust weighting is used to compute a dirty image. The corresponding PSF is exhibited in Figure 1 and its maximum negative sidelobes have a peak of  $-0.068$ , which is 6.8% of the peak value of the PSF. The deconvolution results of the new algorithm are compared to the reconstruction results of the CS-Clean algorithm.

In Figure 2, deconvolution results of the radio M51 image from the new algorithm are depicted. Panels (a) and (c) in Figure 2 are similar, which demonstrates that the new algorithm can effectively recover the original (true) image from the dirty image convolved with the dirty beam. Deconvolution results of the radio image of M31 are displayed in Figure 3 and Figure 4. Visually, both algorithms can effectively recover the original image. This once again verifies that the new algorithm is effective. Experiments indicate that it is often easy for the new algorithm to find a better solution.

Several  $k$  values such as 0.4, 0.6 and 0.8 in the new algorithm are tested, and the change in loop gain is compared to the fixed loop gain in the CS-Clean algorithm. In Figure 5(b), the loop gain in the new algorithm is adaptively changing and monotonically decreasing, which also corresponds to the reconstruction speed shown in Figure 5(a). In the initial phase of deconvolution, the loop gain is large and the signal is extracted quickly. With more in-depth deconvolution, the signal is reduced, the loop gain is reduced and the reconstruction speed is slowed down.

For a more effective comparison, the first 50 iterations of deconvolution and 50 iterations of the same total flux are plotted in Figure 6(a) and 6(b) respectively. As expected, neither algorithm manifested significant oscillation at the beginning of the deconvolution process (see Fig. 6(a)). Figure 6(b) displays the changes in the total flux after 50 iterations with the same reconstruction level. The CS-Clean deconvolution shows oscillations, but the new algorithm does not. As can be seen from Figure 5(b), loop gains of the CS-Clean deconvolution algorithm are the same for all model components. They cannot track the signal amplitude, but the new algorithm can do this. These experiments indicate that the new algorithm can effectively solve the oscillation problem caused by a fixed loop gain.

#### 5 SUMMARY

We introduce a PSNR-based method to improve the CS-Clean deconvolution algorithm. We mathematically provide a way to determine the rate of the steepest descent method. In the new algorithm, the loop gain is adaptively

<sup>3</sup> <http://casa.nrao.edu/>

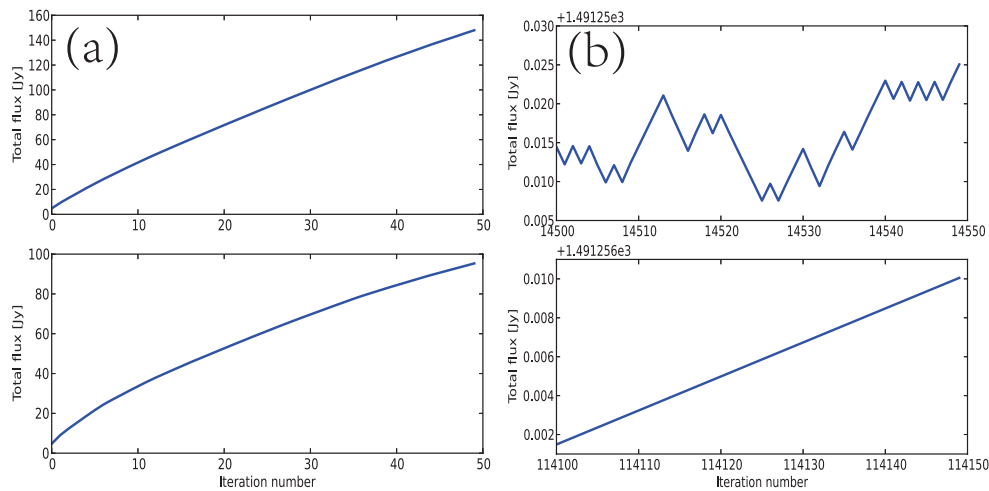


**Fig. 6** This figure shows the changes in the total flux of M31 when deconvolution is applied. (a) The top and bottom panels display the reconstruction speed of model flux with  $g = 0.6$  and  $k = 0.6$  in the first 50 iterations; (b) the top and bottom panels show the reconstructed speed of model flux with  $g = 0.6$  and  $k = 0.6$  in the 50 iterations of the same reconstruction level, respectively. The top panel is from the CS-Clean algorithm while the bottom panel is from the new algorithm.

changed, and the loop gain curve is a good indicator of parameter adjustment. This makes the resulting deconvolution more robust. The improvement comes from more detailed consideration of the data in the deconvolution process. In the future, we will explore other ways and more factors to improve deconvolution algorithms. This work is implemented using Python and with the CASA package.

**Acknowledgements** This work was partially supported by the Open Research Program of the CAS Key Laboratory of Solar Activity (KLSA201805), the Guizhou Science & Technology Plan Project (Platform Talent No.[2017]5788), the Youth Science & Technology Talents Development Project of Guizhou Education Department (No. KY[2018]119), the National Science Foundation of China (Grant Nos. 11103055, 11773062 and 61605153), “Light of West China” Programme (Grant Nos. RCPY201105 and 2017-XBQNXZ-A-008) and the

National Basic Research Program of China (973 program: 2012CB821804 and 2015CB857100).

## References

- Bhatnagar, S., & Cornwell, T. J. 2004, *A&A*, 426, 747  
 Clark, B. G. 1980, *A&A*, 89, 377  
 Cornwell, T. J. 2008, *IEEE Journal of Selected Topics in Signal Processing*, 2, 793  
 Högbom, J. A. 1974, *A&AS*, 15, 417  
 Rau, U., & Cornwell, T. J. 2011, *A&A*, 532, A71  
 Schwab, F. R., & Cotton, W. D. 1983, *AJ*, 88, 688  
 Steer, D. G., Dewdney, P. E., & Ito, M. R. 1984, *A&A*, 137, 159  
 Thompson, A. R., Moran, J. M., & Swenson, Jr., G. W. 2017, *Interferometry and Synthesis in Radio Astronomy* (3rd edn.: Springer)  
 Zhang, L., Zhang, M., & Liu, X. 2016a, *Ap&SS*, 361, 153  
 Zhang, L., Bhatnagar, S., Rau, U., & Zhang, M. 2016b, *A&A*, 592, A128